行政院國家科學委員會補助專題研究計畫成果報告

計畫名稱: 連桿組類型圖的建構與應用

計畫類別：■ 個別型計畫　　□ 整合型計畫
計畫編號：NSC 96-2221-E-034 -011－
執行期間：　96 年 08 月 01 日至　97 年 07 月 31 日

計畫主持人：鐘文遠
共同主持人：
計畫參與人員： 胡育昇、張紹德、賴秀俞

成果報告類型(依經費核定清單規定繳交)：■精簡報告　□完整報告

執行單位：中國文化大學機械工程學系

中　華　民　國　97 年　10 月　15 日

1. 前言及文獻探討

具有一個自由度的連桿組機構為最常用的連桿組，其主要特徵為具有單一的輸入桿及單一的輸出桿。而依其輸入桿及輸出桿能否作完全旋轉，該等機構可分類為：(1) 曲柄搖桿機構。(2) 雙搖桿機構。(3) 雙曲柄機構。如何迅速判別輸入桿及輸出桿能否作完全旋轉，向來為探討連桿組機構之最基本課題之一。

對於平面之四連桿機構，只須將連桿組中各桿之長度，代入一般熟知的 Grashof 氏定理〔Barker, 1985；Paul, 1979〕，便可判別輸入桿或輸出桿能否作完全旋轉。而球面四連桿機構，四根連桿的長度則可更換為連桿間的四個夾角，Grashof 氏定理仍有其適用性〔Chiang, 1988〕。另外，對運動方程式予以分析推導出的判別式〔Murray and Larochelle, 1998〕，亦可用於判別輸入桿或輸出桿能否作完全旋轉。

空間之四連桿機構中，較為簡易且相關研究較多者之一為 RSSR 四連桿機構，描述此機構共需 7 個變數。設計此四連桿機構時，可將除耦桿長度外的尺寸及角度固定，再對連桿組能否連接加以分析〔Freudenstein and Kiss, 1969； Freudenstein and Primrose, 1976；Gupta and Radcliffe, 1971； Suh and Radcliffe, 1978〕，以求得適用之耦桿長度的範圍；但分析過程中須對輸入桿於不同角度時分別運算，因此頗為繁瑣耗時。另外，將描述輸入桿角度及輸出桿角度關係的位置方程式 (Position Equation) 加以分析，可推得一個圓與橢圓方程式之組合，或可推得一個四次方程式，藉由判別式之正負值，以判斷連桿組能否接合或輸出入桿能否完全旋轉〔Nolle, 1969；Lebedev and Tikhonov, 1973；Bottema, 1971; Alizade and Sandor, 1985; Williams and Reinholtz, 1987; Ting and Dou, 1994〕〕。或由極值觀念以分析簡易型之 RSSR 機構〔Zhang and Zhang, 1993〕，可得出 Grashof 氏定理有部分適用性。此外，Jacobian 矩陣〔Litvin, 1980〕、傳動角〔Kazerounian and Solecki, 1993〕及機器人學中之工作空間的概念〔Chung, 2001〕亦可為分析輸入桿或輸出桿能否作完全旋轉之工具。對於桿件可完全旋轉或不可能完全旋轉之充分條件亦被探討分析 [Mallik, 1994; Rastegar and Tu, 1992; Angeles and Bernier, 1987]。而較複雜的 RPSPR 連桿組[DasGupta, 2004]，也可採類似方法加以研究。

然而無論上述的研究成果或一般連桿機構用的軟體，多僅能從事分析工作，因此須待連桿組的所有尺寸確定後，再使用軟體或相關理論以分析其相關性能；當其類型或可運動範圍不符所需，或者傳力角及桿長比等考慮的因素不夠理想時，便得重新選擇另一組連桿組尺寸後再作分析，造成設計過程的耗時及繁瑣，因此上述研究成果及相關軟體對設計連桿組的助益極為有限。相對的，本研究計畫以連桿組的設計合成為主要考量，發展二維及三維的類型圖。以二維類型圖為例，可選擇二個尺寸為座標軸，將連桿組各類型所佔區域於圖上加以分析標示；而在該類型圖上，可繪製如傳力角及桿長比等相關資訊。藉此，可使設計者於適合的類型圖上，迅速的選擇符合需求的區間或點，便可完成連桿之尺寸設計，避免錯誤嘗試的時間浪費。

2. 類型判別

本研究的類型圖建立，主要針對平面四連桿以及 RSSR 簡易四連桿組。有關類型判別以及傳力角等相關理論基礎，於此先加以介紹。連桿組依其輸出入桿能否完全旋轉，其類型共有五種 - 分別為牽桿(Drag-Link 或 C-C)、曲柄搖桿(C-R)、搖桿曲柄(R-C)、雙搖桿(Double-Rocker 或 R-R)及無法連接(NC)等。也代表類型圖上將出現上述五個區域。

2.1 四連桿組

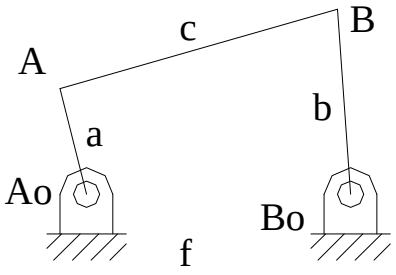

圖一:四連桿組

對於平面四連桿組,若已知各桿尺寸時,可基於 Grashof 氏定理以判別其類型。但 Grashof 氏定理於建構類型圖時，並不易直接套用。建構時乃以附錄一的式(31)為主要依據。如圖一所示的四連桿組，a 為輸入桿，b 為輸出桿，c 為耦桿，f 為機架桿。則輸入桿可完全旋轉的條件為符合式(1)及式(2)

$$(a+b+c-f)(-a+b+c+f)(a+b-c-f)(a-b+c-f)\geq 0 \quad (1)$$

$$(a+b+c+f)(a-b+c+f)(a+b-c+f)(-a+b+c-f)\geq 0 \quad (2)$$

若連桿組的尺寸，符合式(1)及(2)，則該連桿組的輸入桿為可完全旋轉。而符合式(1)及式(2)的區域，則以”I-C”標示。

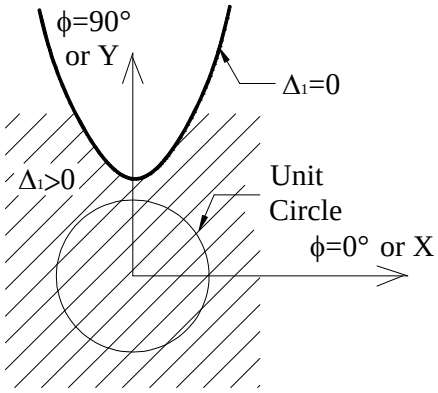

(a). $-C_5\geq 0$ and $(C_2+C_6)/(-C_5)\geq 1$

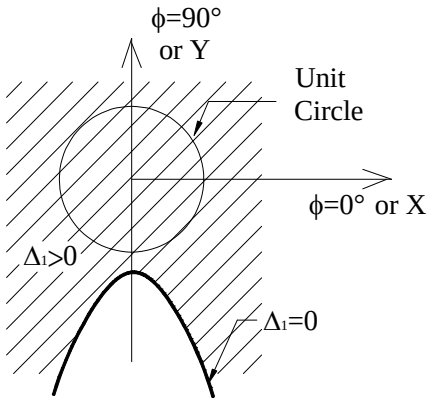

(b) $-C_5\leq 0$ and $(C_2+C_6)/(-C_5)\leq -1$

圖二:當 $C_1\geq C_2$ 的兩狀況

式(1)及(2)的推導是基於附錄一的式(5) $\Delta_1\geq 0$，而如圖二所示的單位圓須完全位於斜線區域內。現若考慮單位圓完全不位於斜線區域內，則此時連桿組的類型為無法連接。因此圖二(a)的拋物線頂點需位於(0, -1)以下，而圖二(b)的頂點則需位於(0，1)以上。仿附錄一的式(12)-(13)，可得

$$C_2+C_6+C_5<0 \quad (3a)$$

$$C_2+C_6-C_5<0 \quad (3b)$$

代入平面四連桿的變數後，則可推得當以下二式皆成立時，連桿組才可能為無法連接。

$$(a+b+c-f)(-a+b+c+f)(a+b-c-f)(a-b+c-f)<0 \quad (4a)$$

$$(a+b+c+f)(a-b+c+f)(a+b-c+f)(-a+b+c-f)<0 \quad (4b)$$

此外，拋物線與單位圓不能有交點。因此附錄一的式(19)也需納入考慮。對於平面四連桿組，

各C_i值分別為

$$C_1 = 4a^2b^2 \qquad C_2 = 4a^2\left(b^2 - f^2\right) \qquad C_3 = C_4 = 0$$

$$C_5 = 2\left(-4ab^2f + 2af \cdot I\right) \qquad C_6 = 4b^2f^2 - I^2 \qquad I = a^2 + b^2 - c^2 + f^2 \tag{5}$$

附錄一的式(19-1)成為$T_1 = 64a^2b^2f^2c^2$，並不成立；因此附錄一的式(19-2)或(19-3)必須成立，此二式可推得為

$$(a^2 - b^2 - c^2 + f^2)^2 - 4a^2f^2 \geq 0 \tag{6}$$

$$-a^4 + (2b^2 + 2f^2 + 2c^2)a^2 + 4b^2f^2 - (f^2 + b^2 - c^2)^2 \leq 0 \tag{7}$$

當連桿組的尺寸，符合式(4a)及(4b)以及式(6)或式(7)任一式，則該連桿組為無法連接。該區域則以”I-N”標示。若連桿組的尺寸，不屬於”I-C”或”I-N” 區域，則輸入桿為不能360^o旋轉的搖桿，該區域則標示”I-R”。

對於式(1)-(7)等式，若將變數 a 及 b 對調，則可適用於輸出桿的類型判別。而可分別得到”O-C”、”O-R”及”O-N”等三區域。

2.2 簡易 RSSR 簡易連桿組

如圖二的 RSSR 四連桿組有六個長度尺寸及輸出入軸線間之夾角，該連桿組不但沒有簡要的判別式以決定其類型，若單以長度尺寸為類型圖的座標軸選擇，便有十五種組合；基於複雜性及可行性的考量，並不適合建構類型圖。

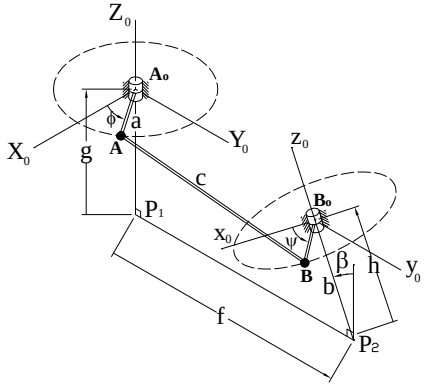

圖二: RSSR 連桿組

至於簡易型的 RSSR 四連桿組，輸出入桿的旋轉中心點皆位於兩軸線的公垂線上，亦即 g=h=0，所以此連桿組僅有 a、b、c 及 f 四個長度尺寸和夾角β。若是針對其輸入桿是否為曲柄，依據附錄一的結果，須分兩部份判別。一為當$f \geq b\left|\sin\beta\right|$時，則須同時符合

$$(a + b + c - f)(-a + b + c + f)(a + b - c - f)(a - b + c - f) \geq 0 \tag{8}$$

$$(a + b + c + f)(a - b + c + f)(a + b - c + f)(-a + b + c - f) \geq 0 \tag{9}$$

而若$f < b\left|\sin\beta\right|$，除了式(8)及式(9)皆須符合外，尚需考慮拋物線與單位圓不能相交；因而另需符合式(10)或式(11)

$$\begin{aligned} &-2\left(a^2b^2 + a^2c^2 + a^2f^2 + b^2c^2 + b^2f^2 + c^2f^2\right)\sin^2\beta \\ &\quad + \left(a^4 + b^4 + c^4 + f^4\right)\sin^2\beta + 4a^2b^2\sin^4\beta + 4c^2f^2 \leq 0 \end{aligned} \tag{10}$$

$$f^2(a^2-b^2-c^2+f^2)^2-4a^2(b^2\sin^2\beta-f^2)^2\geq 0 \tag{11}$$

此外，式(11)亦可由式(12)取代

$$\frac{(a^2+b^2-c^2+f^2)^2+4a^2f^2-4a^2b^2-4b^2f^2}{4a^2\left(f^2-b^2\sin^2\beta\right)}\geq 2 \tag{12}$$

藉由式(8)-(12)，可建立輸入桿為曲柄的區域，亦即"I-C"區。

對於連桿組無法連接區，亦須分兩部份處理。當 $f\geq b|\sin\beta|$ ，除須符合式(13)及(14)外

$$(a+b+c-f)(-a+b+c+f)(a+b-c-f)(a-b+c-f)<0 \tag{13}$$

$$(a+b+c+f)(a-b+c+f)(a+b-c+f)(-a+b+c-f)<0 \tag{14}$$

亦須考慮拋物線與單位圓不能相交。因而另需符合式(10)或式(11)；或者是符合式(10)或式(12)。若 $f<b|\sin\beta|$ ，則只要式(13)及(14)皆符合，連桿組即為無法連接。藉由上述式(10)-(14)及兩部份分析，可建立連桿組無法連接的"I-N"區。

另外，如不屬於"I-C"或"I-N"區域者，該區域代表輸入桿為搖桿，將標示"I-R"。若將式(8)-(14)中的變數 a 及 b 對調，則可適用於輸出桿的類型判別。而可分別得到"O-C"、"O-R"及"O-N" 等三區域。

3. 傳力角與傳力比

傳力比 TR(Transmission ratio)代表耦桿牽動輸出桿的省力程度。求得沿著耦桿的單位向量與沿著輸出桿末端點運動方向的單位向量後，將兩單位向量作內積，即為傳力比 TR 值。當兩單位向量為同向時，TR 值為 1，代表耦桿最能輕易帶動輸出桿。

對於簡易型的 RSSR 四連桿組，TR 值可用下式表示[Kazerounian and Solecki, 1993]

$$TR^2=-Z=-\{A\cos 2\theta+C\cos\theta+E\}/\gamma^2 \tag{15}$$

其中θ為輸入桿角度，且

$$\begin{aligned}A&=2a^2\left(f^2-b^2\sin^2\beta\right)\\ C&=-4af\left(2b^2-H\right)\\ E&=-2a^2\left(b^2+b^2\cos^2\beta-f^2\right)-4b^2f^2+H^2\\ H&=a^2+f^2-c^2+b^2\\ \gamma&=2bc\end{aligned} \tag{16}$$

因為 $\cos 2\theta=2\cos^2\theta-1$ ，式(15)可改寫為

$$TR^2=-\{2A\cos^2\theta+C\cos\theta+E-A\}/\gamma^2 \tag{17}$$

式(17)中，若 $f\geq b|\sin\beta|$ ，則 $A\geq 0$ ，TR^2 對 $\cos\theta$ 的曲線為開口向下。如果 $\cos\theta=-C/4A$ 介於±1間，則 TR^2 於 $\cos\theta=-C/4A$ 時為最大值；當 $\cos\theta=1$ 或 $\cos\theta=-1$ 時，TR^2 為區域最小值。對於 $\cos\theta=-C/4A$ 位於±1間，可表示為

$$f^2(a^2-b^2-c^2+f^2)^2-4a^2(b^2\sin^2\beta-f^2)^2\le 0 \tag{18}$$

以 $\beta=0$ 的平面四連桿組而言，習稱的傳力角為如圖一的 $\mu=\angle ABB_o$，且 $TR^2=1-(\cos^2\mu)$。如圖三(a)所示，為一符合式(18)的平面四連桿組，因此 TR^2 有最大值。且由於 $\beta=0$，當 $\cos\theta=-C/4A$ 時，可證得式(15)中 TR^2 的最大值為 1 或 $\mu=90^o$。反之，當 $\cos\theta=-C/4A$ 不介於 ±1 間；則如圖三(b)所示，TR^2 僅於 $\cos\theta=1$ 或 $\cos\theta=-1$ 時，有區域最小值或區域最大值。如圖四(a)所示為 $\beta=30^o$ 的簡易型 RSSR 四連桿組，因符合式(18)，所以 TR^2 有不等於 1 的最大極值。該極值可表示為

$$TR^{*2}=\frac{1}{4b^2c^2}\left(\begin{array}{l}\dfrac{-f^2\left(b^2+c^2-a^2-f^2\right)^2}{b^2\sin^2\beta-f^2}+2a^2\left(b^2+b^2\cos^2\beta-f^2\right)\\+4b^2f^2-\left(b^2-c^2+a^2+f^2\right)^2-2a^2\left(b^2\sin^2\beta-f^2\right)\end{array}\right) \tag{19}$$

而圖四(b)所示者因式(18)不符合，TR^2 僅於 $\cos\theta=-1$ 時，有區域最大值。

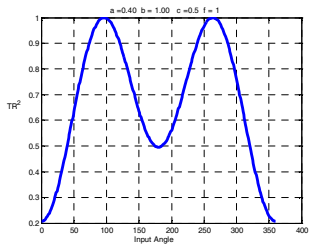

圖三(a) TR^{*2} 有為 1 的極大值

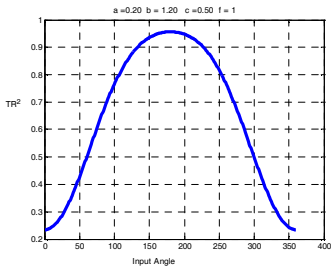

圖三(b) TR^{*2} 沒有為 1 的極值

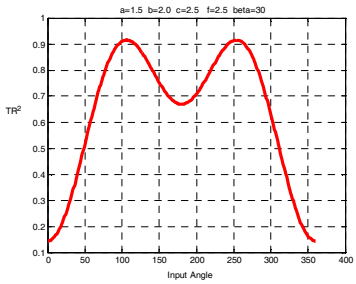

圖四(a) TR^2 有極大值

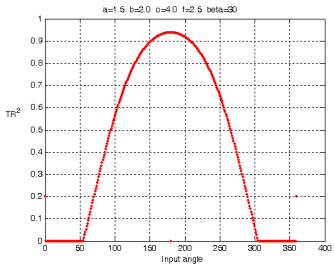

圖四(b) TR^2 沒有極值

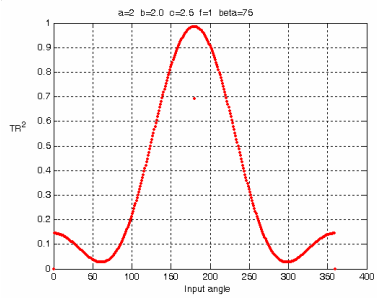

圖五 TR^2 有最小值

當 $f<b|\sin\beta|$，則 $A<0$，TR^2 對 $\cos\theta$ 的曲線為開口向上。若 $\cos\theta=-C/4A$ 介於 ±1 間，則

$\cos\theta = -C/4A$ 時，TR^2 有最小值。如圖五所示即為其中一例；且當 $\cos\theta = 1$ 或 $\cos\theta = -1$ 時，TR^2 為區域最大值。而若 $\cos\theta = -C/4A$ 不介於 ± 1 間時，則 TR^2 僅於 $\cos\theta = 1$ 或 $\cos\theta = -1$ 時，有區域最小值或區域最大值。

4. 平面四連組的類型圖

本節略述平面四連組的類型圖建立及相關應用。利用 2.1 節的式(1)~(7)，可建立如圖六所示的"I-C"、"I-N"及"I-R"等三區。以相似方法，可建立"O-C"、" O -N"及" O -R" 等三區。目前各 3D 繪圖軟體，仍無法直接由方程式建立實體模型。因此，建立時約略須經由以下六步驟:(1) 將如式(1)~(7)的曲面分成數個曲線 (2) 使用如 MATLAB 的數值計算軟體，計算各曲線上若干點的座標數據。 (3)基於該若干點的座標數據，利用如 PRO/E 的 3D 繪圖軟體建立各曲線。 (4) 利用如邊界混成的 3D 繪圖工具，將各曲線結合成曲面。 (5)使用如引伸的工具，建立 3D 實體區塊。 (6) 配合邏輯運作，建立各類型的 3D 實體區塊。

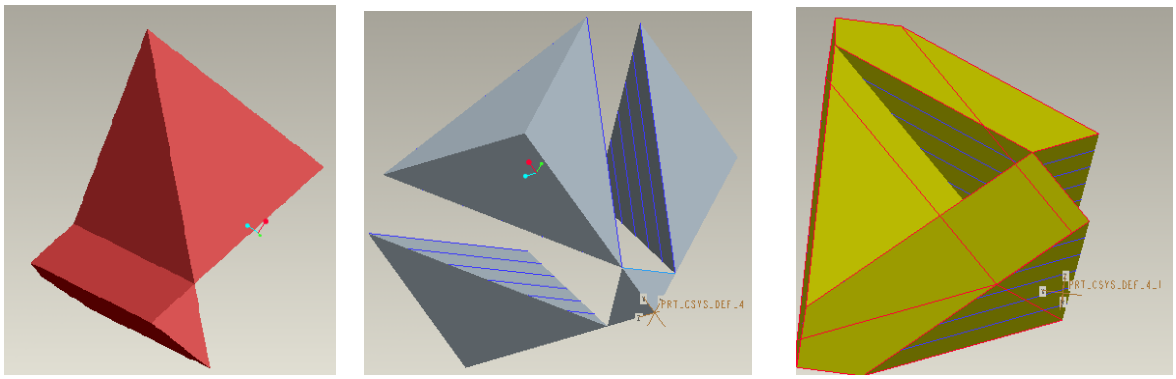

(a) I-C 區　　(b) I-N 區　　(c) I-R 區

圖六: 平面四連組的"I-C"、"I-N"及"I-R"等三區

當建立好上述六區後，可再利用邏輯運作；將 I-C 區與 O-C 區交集得 Drag-Link 或 C-C 區，將 I-C 區與 O-R 區 交集得 crank-rocker 或 C-R 區，將 I-R 區 與 O-C 區 交集得 rocker-crank 或 R-C 區，將 I-R 區 與 O-R 區 交集得 double rocker 或 R-R 區。至於無法連接區則與 I-N 區或 O-N 區完全相同。其結果如圖七所示。

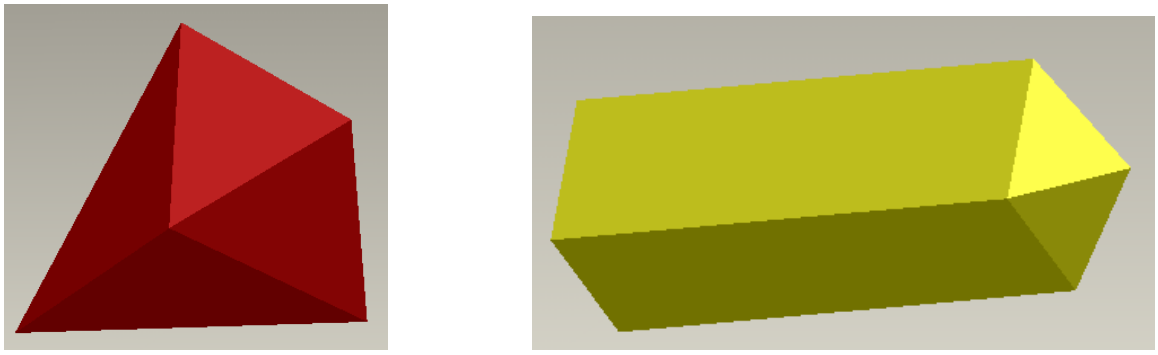

(a) Drag-Link 區　　(b)crank-rocker 區

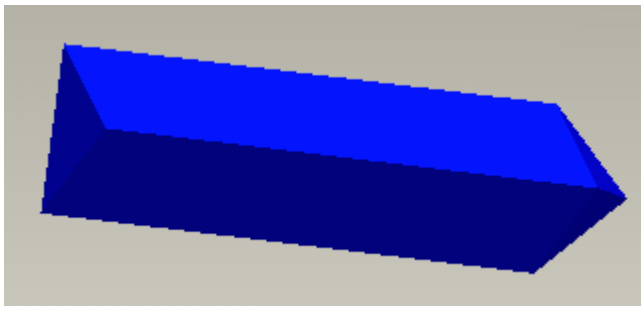

(c)rocker-crank 區

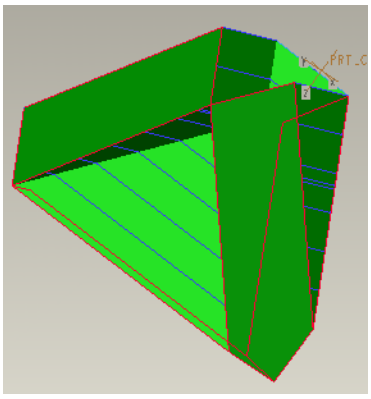

(d) double rocker 區

圖七: 平面四連組的四種類型

該等類型圖的功用，可基於設計的考量，而有不同的應用方式。前述的圖六~七，其 x、y 及 z 分別代表輸入桿、耦桿及輸出桿對固定桿的桿長比值。例如設計的需求若為合成雙搖桿或曲柄搖桿機構時，則可將圖七(a)及圖七(b)加以組合，得到如圖八(a)的 3D 模型。其中紅色區塊為雙搖桿，黃色區塊為曲柄搖桿。設計者因而能於適當的區塊指定任一點，以合成連桿組。設若再指定耦桿對固定桿的桿長比值，亦即指定 y 的值；則可於圖八(a)作垂直於 y 軸的剖面。該等剖面可由不同角度加以查看，如圖八(b)為從 y 軸方向查看，所以設計課題簡化為於 2D 平面上選擇適當點。而剖面方式可依設計需求而定，如圖九所示其剖面不與任何座標軸垂直；圖九(b)則顯示設計課題也可簡化為在 2D 平面上選擇適當點。

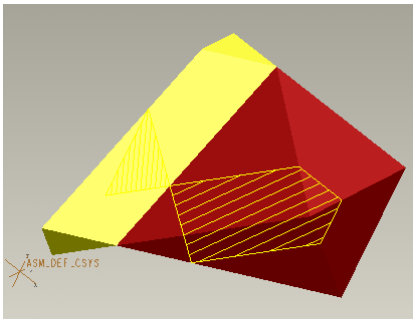

(a) 一般 3D 圖示

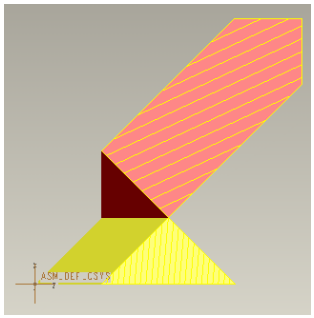

(b)垂直於剖面視角

圖八: 平面四連組的應用例

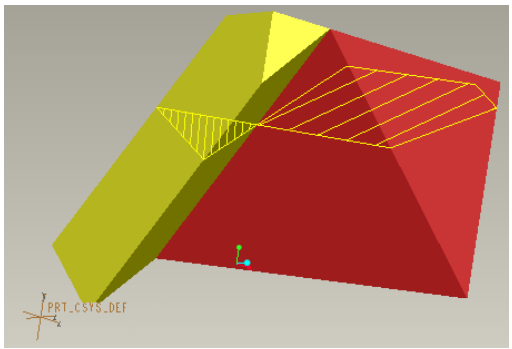

(a) 一般 3D 圖示

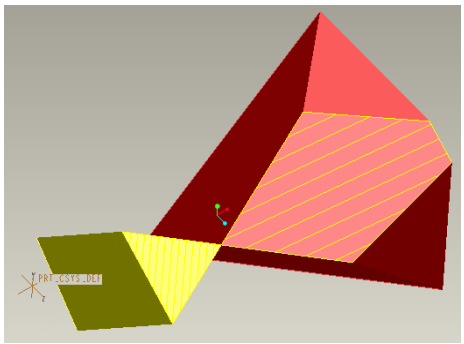

(b)垂直於剖面視角

圖九: 平面四連組的應用例

類型圖亦可加入第 3 節的傳力角以輔助設計。如圖十所示，加入最小傳力角為 30 度與 60 度的曲線、最大傳力角為 120 度、135 度與 150 度的曲線、及式(18)的曲線。以圖上 A、B 及

C 三點而言，其耦桿及輸出桿對固定桿的桿長比值皆為 2，輸入桿對固定桿的桿長比值分別約為 2、1.5 及 2.5。A 及 C 點因位於符合式(18)的區域，可知有最佳傳力角 90°。A 及 C 點兩者的最大傳力角皆小於 120°，且點 A 更優於點 C，或更近於 90°。最小傳力角部份，點 A 約為 30°，點 C 約為 45°。因此以傳力角而言，三點中應以點 C 所代表的尺寸為最佳選擇。

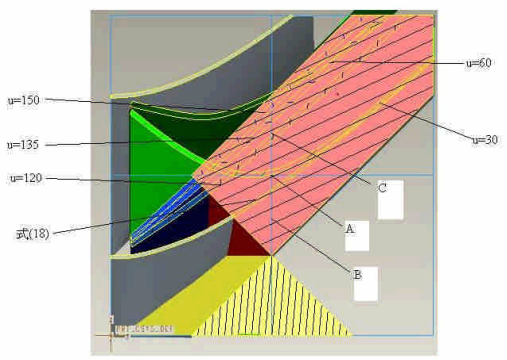

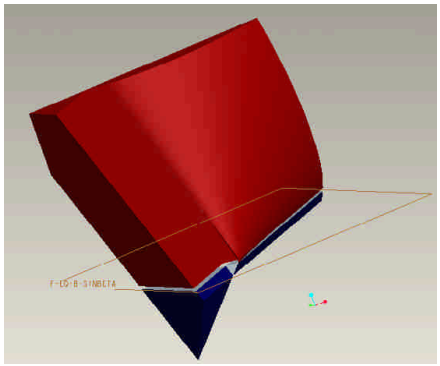

圖十: 平面四連組考慮傳力角的應用例　圖十一: 簡易 RSSR$\beta = 60^{o}$輸入桿為搖桿的區塊

5. RSSR 簡易四連桿組的類型圖

RSSR 簡易四連桿組的類型圖建立，較平面四連組繁複且耗時很多。主要有兩個原因: 一為須依$f \geq b|\sin\beta|$ 或$f < b|\sin\beta|$ 分兩段考量；另一為不似平面四連組，其類型由各平面所切割，而其類型乃是由如式(10)及(12)等複雜曲面為邊界。如圖十一所示為如圖二的$\beta = 60^{o}$，且輸入桿為搖桿的區塊，亦即前述的”I-C”區。若仍以 x、y 及 z 分別代表輸入桿、耦桿及輸出桿對固定桿的桿長比值，則$f = b|\sin\beta|$代表$z = 1.1547$。圖中藍色為$f \geq b|\sin\beta|$的區域，紅色區域為$f < b|\sin\beta|$的區域。藍色區域如同平面四連桿，但紅色區域部分，可看出其邊界皆為複雜的曲面。

”O-C”區可如同建構”I-C”區的方式加以建構。再將兩者合併並做邏輯操作後，可得到如”C-C”、”C-R”及”R-C”等區域。若將該三個區域合併，藉由 3D 繪圖軟體的剖面功能，可得到如圖十二的各個任意剖面。因此如圖八(b)及九(b)般，設計者僅需於 2D 剖面上選擇適當點，便可完成設計。當然，類型圖亦可依設計需求，加入如圖十三所示的傳力比相關曲面，以輔助設計。圖十三的紅、黃、綠三個曲面，分別代表式(19)的TR^{*2}等於 0.25、0.50 及 0.75。

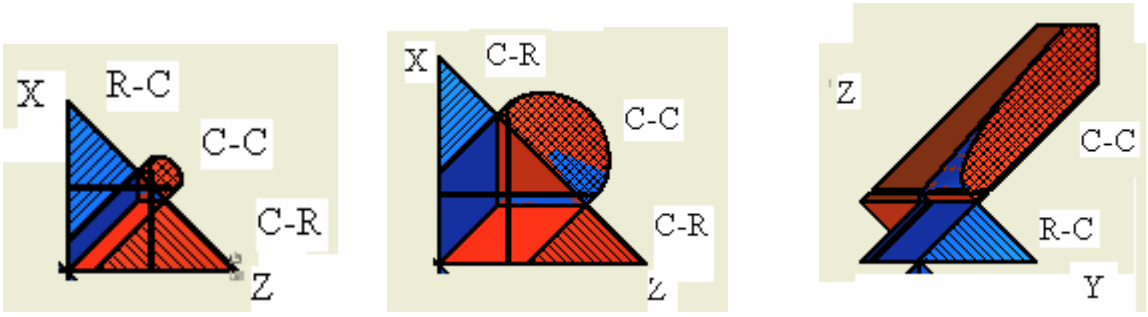

(a)Y 為較小定值的剖面　(b) Y 為較大定值的剖面　(c) X 為定值的剖面

圖十二: 簡易$\beta = 60^{o}$ RSSR 的剖面類型圖

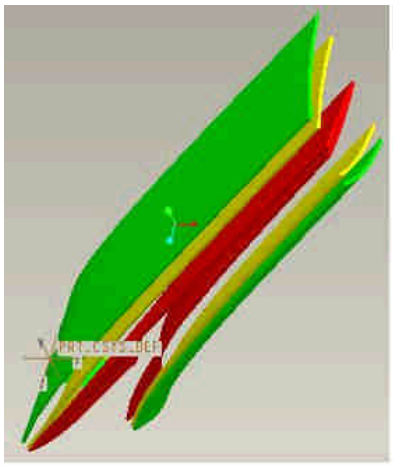

圖十三: 傳力比相關曲面

6. 討論及結論

本研究計畫由推導判別類型的不等式為起始，再利用相關數值軟體及 3D 設計軟體，建構立體的類型圖。主要應用於當連桿組的四個長度為待定尺寸時，可將其中三桿與第四桿的桿長比當做立體圖的座標軸。立體類型圖再輔以相關設計需求的曲面後，根據所欲設計的連桿組類型、傳力比及其他需求，可於 3D 環境或 2D 截面，選擇適當點以迅速得完成設計。

本計畫執行時，3D 設計軟體仍無法根據給定的方程式直接建構曲面。類型圖的建構需藉由如 MATLAB 的數值軟體，求得多點的座標數據後，再逐步建立曲線、曲面及實體，程序頗為煩雜費時。倘若未來 3D 設計軟體可依給定的方程式直接建構曲面，將使 3D 類型圖的建立變為迅速簡易。此外，當 3D 類型圖及相關設計需求的曲面建立後，可再與虛擬實境配合。則設計者於決定連桿組的待定桿長尺寸時，便有如人類於實際生活中，在 3D 環境中執行物體的取放；可大幅降低設計的難度。

參考文獻:

1. Angeles, J. and Bernier, 1987, "A General Method of Four-Bar Linkage Mobility Analysis," Transaction of the ASME, Journal of Mechanisms, Transmissions, and Automation in Design, Vol. 109, pp. 197-203.
2. Alizade, R. I. and Sandor, G. N., 1985, “Determination of the Condition of Existence Complete Crank Rotation and of the Instantaneous Efficiency of Spatial Four-Bar Mechanisms,” Mechanism and Machine Theory, Vol. 20, No. 3, pp. 155-163.
3. Barker, C. R., 1985, "A Complete Classification of Planar Four-Bar Linkages," Mechanism and Machine Theory, Vol. 20, No. 6, pp. 535-554.
4. Bottema, O., 1971, "The Motion of the Skew Four-Bar," Journal of Mechanisms, Vol. 6, pp. 69-79.
5. Chiang, C. H., 1988, Kinematics of Spherical Mechanisms, Cambridge University Press.
6. Chung, W. Y., 2001, "Mobility Analysis of RSSR Mechanisms by Working Volume," DETC2001/DAC-21045, ASME 2001 Design Engineering Technical Conferences.
7. Chung, W. Y., 2004, "Mobility Analysis of RSSR Linkage and Type Maps of Special Cases," Mechanism and Machine Theory, Vol. 39, No. 4, pp. 379-393.
8. Chung, W., 2007, “Analysis of mobility region and type determination for bimodal linkages,”

submitted to 2007 IFToMM World Congress (has been conditionally accepted for presentation during an oral session).

9. DasGupta, A., 2004, “Mobility Analysis of a Class of RPSPR Kinematic Chains,” Transaction of the ASME, Journal of Mechanical Design, Vol. 126, pp. 71-78.
10. Freudenstein, F. and Kiss, I., 1969, "Type Determination of Skew Four-Bar Mechanisms," Transaction of the ASME, Journal of Engineering for Industry, pp. 220-224.
11. Freudenstein, F. and Primrose, E., 1976, "On the Criteria for the rotatability of the Cranks of Skew Four-Bar Linkage," Transaction of the ASME, Journal of Engineering for Industry, pp. 1285-1288.
12. Gupta, V. and Radcliffe, C., 1971, "Mobility Analysis of Plane and Spatial Mechanisms," Transaction of the ASME, Journal of Engineering for Industry, pp. 125-130.
13. Kazerounian, K. and Solecki, R., 1993, "Mobility Analysis of General Bi-Modal Four-Bar Linkages Based on Their Transmission Angle," Mechanism and Machine Theory, Vol. 28, No. 3, pp. 437-445.
14. Lebedev, P. and Tikhonov, N., 1973, "Application of Boolean Algebra to the Analysis of he Position Function of the Spatial Four-Bar Linkage," Mechanism and Machine Theory, Vol. 8, pp. 533-541.
15. Litvin, F., 1980, "Application of Theorem of Implicit Function System Existence for Analysis and Synthesis of Linkages," Mechanism and Machine Theory, Vol. 15, pp. 115-125.
16. Mallik, A. K., 1994, “Mobility Analysis and Type Identification of Four-Link Mechanisms,” Transaction of the ASME, Journal of Mechanical Design, Vol. 116, pp. 629-633.
17. Murray, A. and Larochelle P., 1998, "A Classification Scheme for Planar 4R, Spherical 4R, and Spatial RCCC Linkages to Facilitate Computer Animation," DETC98/MECH-5887, ASME Design Engineering Technical Conferences.
18. Nolle, H., 1969, "Ranges of Motion Transfer by the R-G-G-R Linkage," Journal of Mechanisms, Vol. 4, pp. 145-157.
19. Paul, B., 1979, "A Reassessment of Grashof's Criterion," Transactions of the ASME, Journal of Mechanical Design, Vol. 101, pp. 515-518.
20. Rastegar, J. and Tu, Q. 1992, “Approximated Grashof-Type Movability Conditions for RSSR Mechanisms with Force Transmission Limitations,” Transactions of the ASME, Journal of Mechanical Design, Vol. 114, pp. 74-81.
21. Suh, C. H. and Radcliffe, C. W., 1978, Kinematics and Mechanisms Design, John Wiley & Sons.
22. Ting, K.L. and Dou, X., 1994, "Branch, Mobility Criteria, and Classification of RSSR and Other Bimodal Linkages", ASME Mechanisms Conference: Mechanism Synthesis and Analysis, DE-70, pp. 303-310.
23. Williams, R. L. and Reinholtz, C. F., 1987 "Mechanism Link Rotatability and Limit Position Analysis Using Polynomial Discriminants," Transactions of the ASME, Journal of Mechanisms, Transmissions, and Automation in Design, Vol. 109, pp. 178-182.
24. Zhang, W. and Zhang D., 1993, "Conditions of Crank Existence for a Particular Case of the RSSR Linkage," Mechanism and Machine Theory, Vol. 28, No. 6, pp. 845-850.

附錄一: Chung, W. Y., "Type determination and analysis of mobility region for bimodal linkages," accepted by Proceedings of the Institution of Mechanical Engineers, Part C, Journal of Mechanical Engineering Science. (SCI, EI).

Abstract

A bimodal linkage has two potential output angles for any given input angle, and vice versa. The analysis treats all bimodal linkages as a common problem. A conic curve is derived from the general input-output equation. The mobility regions of any concerned link are then attained from the intersection points between the conic curve and a unit circle with the aid of corresponding differentiation. The linkages with one axis of the conic curve passing through the origin are classified as a selective group. The concise criteria for type determination are shown to be existent for this group, and the strategies to derive them straightforwardly are developed. Unlike Grashof's rule is only applicable to planar four-bar, the criteria developed can be used to determine the type efficiently for all linkages belonging to this selective group and are certainly preferable. The linkages with prismatic output are also considered. Several examples including RPSPR, RPSC, RSSR, and RSSP linkages are given for illustration.

1. Introduction

A bimodal linkage is generally defined that it has two potential output angles for any given input angle and vice versa [1]. Numerous well-known mechanisms, such as planar four-bar, spherical four-bar, spatial RSSR and RPSPR linkage, belong to bimodal linkages. Although deriving criterion to determine the type of a linkage or whether a concerned link can make fully rotation is one of the fundamental issues, only few linkages have been worked out successfully. The type of a planar four-bar is determined by using Grashof's rule [2]. With the aid of the characteristic of supplementary linkages, Grashof's rule is applicable to spherical four-bar linkage [3]. RSSR linkage with zero offsets [4] is the only spatial linkage of which the type determination criteria have been worked out successfully [5-6].

Because deriving type determination criteria for spatial bimodal linkages can hardly be accomplished, determining the mobility region directly or deriving sufficient conditions was usually attempted instead. For RSSR linkage, the concept of relative motion [7-8] and analyzing the input-output equation or the equation of transmission angle have been tried to obtain a quartic equation or an ellipse as well as a circle [9-11]. Therefore, the discriminants of a quartic equation can be treated as the criteria to determine the type [1, 9, 11], but they are too complicated to be applied. For the purpose of designing a linkage, the concept of mobility chart was proposed [12-14]. The zones of nonexistence of double-crank and crank-rocker or existence of crank-rocker and drag-link mechanism were also demarked or derived [15-17]. The RPSPR linkage was analyzed based on the relationship between a circle and a hyperbola or an ellipse [18]. Although these results derived [15-18] are more concise than the discriminants of quartic equation, they are just sufficient conditions.

The derivation of aforementioned literatures mostly focused on a single linkage and the applicability of the results is limited. Besides, the genuine concise criteria for type determination [1-3, 5-6] are individually applicable to planar four-bar, spherical four-bar, or RSSR with zero offsets. In this article, a general strategy to efficiently determine the mobility regions numerically is proposed in Section 2. The results are thus general and applicable to lots of bimodal linkages. A selective group of bimodal linkages that do have concise criteria to determine the type efficiently is classified in Section 3. The strategies to derive criteria straightforwardly are also developed successfully. The favorable criteria can thus be treated as generalized Grashof's rule with applications illustrated in Sections 4 and 5.

2. Analysis of mobility region

Instead of considering only a specified linkage, e.g. RSSR [1, 11] or RPSPR [18], the general

input-output equation applicable to lots of bimodal linkage can be expressed as

$$(A\cos\phi + B\sin\phi + C)\cos\psi + (D\cos\phi + E\sin\phi + F)\sin\psi + G\cos\phi + H\sin\phi + I = 0 \quad (1)$$

The variables ϕ and ψ represent the input and output angles, respectively. All other parameters, such as A, B, .. and I, are constant and related to the dimensions of the linkage. For a given input angle ϕ, none or two real solutions for the output angle ψ can be solved from the equation

$$U_1\cos\psi + V_1\sin\psi + W_1 = 0 \quad (2)$$

where

$$U_1 = A\cos\phi + B\sin\phi + C$$
$$V_1 = D\cos\phi + E\sin\phi + F$$
$$W_1 = G\cos\phi + H\sin\phi + I \quad (3)$$

The sufficient and necessary condition for the existence of real solution of ψ is

$$\Delta_1 \equiv U_1^2 + V_1^2 - W_1^2 \geq 0 \quad (4)$$

After substituting Equations (3) into Equation (4), Δ_1 can be expressed as

$$\Delta_1 = C_1\cos^2\phi + C_2\sin^2\phi + C_3\cos\phi\sin\phi + C_4\cos\phi + C_5\sin\phi + C_6 \geq 0 \quad (5)$$

where

$$C_1 = A^2 + D^2 - G^2 \qquad C_4 = 2(AC + DF - GI)$$
$$C_2 = B^2 + E^2 - H^2 \qquad C_5 = 2(BC + EF - HI)$$
$$C_3 = 2(AB + DE - GH) \qquad C_6 = C^2 + F^2 - I^2 \quad (6)$$

All the values of C_i are constant, and the only variable in Equation (5) is ϕ.

Two steps are proposed to find the mobility region for angle ϕ where $\Delta_1(\phi) \geq 0$ is satisfied. Firstly, the limiting angles ϕ_{lim} satisfying $\Delta_1(\phi_{lim}) = 0$ are to be found. As shown in Figure 1, ϕ_{lim}, such as ϕ_{lim1} and ϕ_{lim2}, are the intersection points between the conic curve $\Delta_1(\phi) = 0$ and a unit circle after setting $X = \cos\phi$ and $Y = \sin\phi$. Besides, combining a conic curve and a circle can lead to a quartic equation and there are four real solutions at most for ϕ_{lim}.

The second step is to find the sign of $d\Delta_1/d\phi$ at each limiting angle ϕ_{lim} by using

$$\frac{d\Delta_1}{d\phi} = 2(-C_1 + C_2)\cos\phi\sin\phi + C_3(\cos^2\phi - \sin^2\phi) - C_4\sin\phi + C_5\cos\phi \quad (7)$$

If $d\Delta_1/d\phi|_{\phi=\phi_{lim1}}$, as shown in Figure 1, is positive, this implies the linkage can be assembled at $\phi = \phi_{lim1} + \delta\phi$ since $\Delta_1(\phi_{lim1} + \delta\phi) > 0$. The term $\delta\phi$ represents a small variation of ϕ. Similarly, the linkage can be assembled at $\phi = \phi_{lim2} - \delta\phi$ if $d\Delta_1/d\phi|_{\phi=\phi_{lim2}} < 0$.

Based on the solved values of ϕ_{lim} and signs of $d\Delta_1/d\phi|_{\phi=\phi_{lim}}$, the mobility region, such as the arc drawn by bold line, of the input link can be determined. The sign of Δ_1 is always positive or always negative if there is no real solution for ϕ_{lim}. The input link is a crank for $\Delta_1 > 0$, and the linkage cannot even be assembled if $\Delta_1 < 0$. The sign of Δ_1 can be verified by various simple tests, such as checking the sign of $\Delta_1 = C_1 + C_4 + C_6$ at $\phi = 0^o$.

When the mobility region of the output link is considered, Equation (1) can be collected as

$$(A\cos\psi + D\sin\psi + G)\cos\phi + (B\cos\psi + E\sin\psi + H)\sin\phi + C\cos\psi + F\sin\psi + I = 0 \quad (8)$$

Similarly, the function $\Delta_2(\psi)$ as in Equation (5) can be derived and the coefficients as in Equation (6) are

$$\hat{C}_1 = A^2 + B^2 - C^2 \qquad \hat{C}_4 = 2(AG + BH - CI)$$

$$\hat{C}_2 = D^2 + E^2 - F^2 \qquad \hat{C}_5 = 2(DG + EH - FI)$$
$$\hat{C}_3 = 2(AD + BE - CF) \qquad \hat{C}_6 = G^2 + H^2 - I^2 \tag{9}$$

The limiting angles $\psi_{\lim}$ are found by combining $\Delta_2 = 0$ and unit circle. The mobility region of the output link can then be figured out by considering the signs of $d\Delta_2 / d\psi \,|_{\psi=\psi_{\lim}}$.

3. Criteria for type determination

The derivation of concise criteria for type determination is dependent on whether the roots of conic curve $\Delta_1 = 0$ or $\Delta_2 = 0$ do exist. Two special cases when $C_3 = C_4 = 0$ and $C_3 = C_5 = 0$ are first focused. When $C_3 = C_4 = 0$, Equation (5) is modified by subtracting $C_2\left(\cos^2\phi + \sin^2\phi - 1\right)$ and becomes

$$(C_1 - C_2)\cos^2\phi \geq -C_5 \sin\phi - (C_2 + C_6) \tag{10}$$

or

$$(C_1 - C_2)X^2 \geq -C_5 Y - (C_2 + C_6) \tag{10'}$$

This inequality represents a region related to a parabola with the axis along the Y-axis. Since this parabola has only one vertex at $\left(0, -(C_2 + C_6)/C_5\right)$, it is favorable for the analysis. Two conditions $C_1 \geq C_2$ and $C_1 < C_2$ are analyzed respectively as follows.

For the condition $C_1 \geq C_2$, Equation (10') can be rewritten as

$$X^2 \geq \frac{-C_5}{C_1 - C_2}\left(Y - \frac{C_2 + C_6}{-C_5}\right) \tag{11}$$

The described region is the outside of the parabola. Two possibilities ensuring that the whole unit circle lies in the described region are shown in Figure 2. For Figure 2(a), $-C_5 \geq 0$ and the vertex must be above (0, 1), the inequality can be obtained as

$$C_2 + C_6 \geq -C_5 \geq 0 \tag{12}$$

The other one is shown in Figure 2(b) when $-C_5 \leq 0$. The vertex is below (0, -1), and the inequality is

$$0 \geq -C_5 \geq -(C_2 + C_6) \tag{13}$$

Both Equations (12) and (13) can be combined to get the necessary and sufficient condition for the existence of crank as

$$C_2 + C_6 + C_5 \geq 0 \tag{14-1}$$
$$C_2 + C_6 - C_5 \geq 0 \tag{14-2}$$

Besides, Equations (14) remain applicable to the special condition $C_1 = C_2$.

For the second condition $C_1 < C_2$, Equation (10') becomes

$$X^2 \leq \frac{-C_5}{C_1 - C_2}\left(Y - \frac{C_2 + C_6}{-C_5}\right) \tag{15}$$

Two cases shown in Figures 3(a) and 3(b) ensure the whole unit circle being within the described region. Since the vertex must locate outside the unit circle, Equations (14) have to be satisfied as well. Besides, the parabola cannot intersect with the unit circle becomes the additional constraint. To simplify the analysis, the equation of the parabola is expressed as

$$X^2 = PY + Q \tag{16}$$

where

$$P = \frac{-C_5}{C_1 - C_2} \quad \text{and} \quad Q = \frac{C_2 + C_6}{C_2 - C_1} \tag{17}$$

By combining Equation (16) with $X^2 + Y^2 = 1$, this leads to

$$X^2 = \left(2Q - P^2 \pm \sqrt{P^2\left(P^2 - 4Q + 4\right)}\right)\Big/2 \tag{18}$$

The parabola doesn't intersect with the unit circle or the variable X has no real roots if $T_1 = P^2 - 4Q + 4 < 0$ or $T_2 = 2Q - P^2 + \sqrt{P^2\left(P^2 - 4Q + 4\right)} < 0$. Besides, the satisfaction of Equations (14) implies $T_3 = P^2 - Q^2 \le 0$ and $Q \ge 0$. All these constraints are shown in Figure 4 for the purpose of analysis. There are two significant features that should be noted. One is that both $T_1 = P^2 - 4Q + 4 = 0$ and $T_3 = P^2 - Q^2 = 0$ are tangent to each other at points (2, 2) and (-2, 2). The other feature is that both $T_2 = 0$ and $T_3 = 0$ are coincident at $|P| \ge 2$ or $Q \ge 2$. As a result, the region $Q \ge 0$ can be divided into four different regions for analyzing with the aid of Table 1.

Region I: This region implies $|P| > Q > 0$ and $T_3 > 0$. Equations (14) is thus unsatisfied.

Region II: This region stands for $T_1 = P^2 - 4Q + 4 < 0$. Since the variable X has no real roots and $T_3 \le 0$, the results as shown in Figures 3(a) and 3(b) can be expected and the link considered can make fully rotation.

Region III: This region is bounded by $T_3 = P^2 - Q^2 \le 0$, $T_1 = P^2 - 4Q + 4 > 0$ and $Q \ge 2$. Since $T_2 \le 0$ is satisfied, the link can be a crank.

Region IV: This region is bounded by $T_3 = P^2 - Q^2 \le 0$, $T_1 = P^2 - 4Q + 4 > 0$ and Q<2. However, the variable X has real solutions due to $T_2 > 0$.

Accordingly, the regions for existence of crank are II and III, and the additional constraint is just one of the following

$$T_1 = {C_5}^2 - 4\left(C_2 + C_6\right)\left(C_2 - C_1\right) + 4\left(C_2 - C_1\right)^2 \le 0 \tag{19-1}$$

$$P^2 = {C_5}^2 \big/ \left(C_1 - C_2\right)^2 \ge 4 \tag{19-2}$$

$$Q = \left(C_2 + C_6\right)\big/\left(C_2 - C_1\right) \ge 2 \tag{19-3}$$

Meanwhile, each inequality of Equations (19) is a sufficient condition. The union of Equations (19-1) and (19-2) or (19-1) and (19-3) becomes the sufficient and necessary condition.

The cases with one axis of the conic curve passing through the origin point are then discussed. By rotating the coordinate with half of angle $\tan^{-1}\left(C_3 \big/ \left(C_1 - C_2\right)\right)$, the new coefficient $\underline{C_3}$ within the modified equation of the conic curve becomes zero. For one axis of the conic curve passes through the origin, either $\underline{C_4}$ or $\underline{C_5}$ is also zero and either Equation (20) or (21) is satisfied.

$$C_4 S_1 + \tau C_5 S_2 = 0 \tag{20}$$

$$C_4 S_2 - \tau C_5 S_1 = 0 \tag{21}$$

where

$$\tau = \text{sign}\left(C_3 \big/ \left(C_1 - C_2\right)\right)$$

$$S_1 = \sqrt{\sqrt{\left(C_1 - C_2\right)^2 + {C_3}^2} + \left|C_1 - C_2\right|}$$

$$S_2 = \sqrt{\sqrt{\left(C_1 - C_2\right)^2 + {C_3}^2} - \left|C_1 - C_2\right|} \tag{22}$$

Therefore, the coefficients of a conic equation can be modified as $\underline{C_3} = \underline{C_4} = 0$ or $\underline{C_3} = \underline{C_5} = 0$ by coordinate rotation whenever Equation (20) or (21) is satisfied. Since the equation of unit circle remains the same after coordinate rotation, the technique for $C_3 = C_4 = 0$ or $C_3 = C_5 = 0$ can then be applied to derive the concise criteria for type determination.

One special case should be noted is when $C_3 = 0$ and $C_1 = C_2$. Evidently, the conic curve is just a circle and Equations (20) and (21) are both satisfied. Moreover, Equation (5) represents the

region with a straight line as boundary and becomes

$$\Delta_1 = C_4 \cos\phi + C_5 \sin\phi + C_6 + C_1 \geq 0$$

Hence, the condition for existence of crank is just

$$C_6 + C_1 \geq \sqrt{{C_4}^2 + {C_5}^2} \tag{23}$$

The case $C_3 = 0$ implies two axes of the conic curve being parallel to X-axis and Y-axis. If similar technique as in Figure 4 and Equation (16) is applied, the parabola equation becomes $(X + R)^2 = PY + Q$ and has three parameters. Hence, the analysis as in Table 1 cannot be followed since a tedious three-dimension problem will be met up. Although several sufficient conditions for the existence of crank might be attained as in [18], the advantage when compared with quartic discriminants is debatable. Consequently, if the case $C_3 = 0$ or even general case $C_3 \neq 0$ is considered, solving the mobility region by following the strategy proposed in Section 2 is suggested with the dimensions of the linkages being assigned.

The analysis in this Section discloses that a selective group of bimodal linkage does have concise criteria for type determination. The feature is that one axis of the conic curve passes through the origin. Three special cases among this group are $C_3 = C_4 = 0$, $C_3 = C_5 = 0$, and $C_1 - C_2 = 0 = C_3$. A flowchart is proposed in Figure 5 to illustrate the derivation of concise type determination criteria. The Equation number with * sign, e.g. (14-1)* or (19-1)*, represents that C_1 and C_5 have to be swapped by C_2 and C_4 respectively. Accordingly, this flowchart works as "standard derivation strategy" and the derivation is straightforward.

4. Analysis of RPSPR linkage

A general RPSPR is dismantled into two manipulators R_1P_1 and R_2P_2 for analysis, and both are set on fixed frames $X_0 - Y_0 - Z_0$ and $x_0 - y_0 - z_0$ as shown in Figure 6. Points O and o are origins, and Y_0 axis is parallel to y_0 axis. The skewed angle and distance between Z_0 and z_0 axes are β and f. The offsets are $\overline{ON} = g$ and $\overline{on} = h$. The Denavit-Hartenberg notation $(a_{i-1}, \alpha_{i-1}, d_i, \theta_i)$ [19-20] and moving frames $X_i - Y_i - Z_i$ (i=1 and 2) are used to describe the R_1P_1 manipulator, while $(b_{i-1}, \gamma_{i-1}, e_i, \tau_i)$ and frames $x_0 - y_0 - z_0$ (i=1 and 2) are for the R_2P_2 manipulator. Among all 16 parameters, a_0, α_0, d_1, θ_2, b_0, γ_0, e_1 and τ_2 are zero, and a_1, α_1, b_1 and γ_1 are related to the dimension of the linkage. The variables θ_1 and τ_1 are the input angle ϕ and output angle ψ. Two other variables are d_2 and e_2. The coordinate of the point S with respect to the frame $X_2 - Y_2 - Z_2$ is defined as ${}^2\mathbf{S_{XYZ}} = [S_X, S_Y, S_Z]^T$, and is ${}^2\mathbf{S_{xyz}} = [S_x, S_y, S_z]^T$ with respect to frame $x_2 - y_2 - z_2$.

The coordinates of the S joint with respect to two fixed frames are thus

$${}^0\mathbf{S_{XYZ}} = (a_1 + S_X)\mathbf{I_1} + S_Y\mathbf{J}_2 + (S_Z + d_2)\mathbf{K}_2 \tag{24}$$

$${}^0\mathbf{S}_{xyz} = (b_1 + S_x)\mathbf{i_1} + S_y\mathbf{j_2} + (S_z + e_2)\mathbf{k_2} \tag{25}$$

where

$$\mathbf{I_1} = \mathbf{I_2} = [\cos\theta_1, \sin\theta_1, 0]^T$$

$$\mathbf{J_2} = [-\cos\alpha_1 \sin\theta_1, \cos\alpha_1 \cos\theta_1, \sin\alpha_1]^T$$

$$\mathbf{K_2} = [\sin\alpha_1 \sin\theta_1, -\sin\alpha_1 \cos\theta_1, \cos\alpha_1]^T$$

$$\mathbf{i_1} = \mathbf{i_2} = [\cos\tau_1, \sin\tau_1, 0]^T$$

$$\mathbf{j_2} = [-\cos\gamma_1 \sin\tau_1, \cos\gamma_1 \cos\tau_1, \sin\gamma_1]^T$$

$$\mathbf{k_2} = [\sin\gamma_1 \sin\tau_1, -\sin\gamma_1 \cos\tau_1, \cos\gamma_1]^T$$

Besides, ${}^{0}\mathbf{S}_{\mathbf{XYZ}}$ and ${}^{0}\mathbf{S}_{xyz}$ can be related by

$$ {}^{0}\mathbf{S}_{\mathbf{XYZ}} = \mathbf{T}\,{}^{0}\mathbf{S}_{\mathbf{xyz}} + \mathbf{P} \tag{26} $$

where

$$ \mathbf{T} = \begin{bmatrix} \cos\beta & 0 & \sin\beta \\ 0 & 1 & 0 \\ -\sin\beta & 0 & \cos\beta \end{bmatrix} \text{ and } \mathbf{P} = \begin{bmatrix} h\sin\beta \\ f \\ h\cos\beta - g \end{bmatrix} \tag{27} $$

After substituting Equations (24) and (25), Equation (26) can be expanded as

$$ [\mathbf{M} \quad \mathbf{K}_2 \quad \mathbf{Tk_2}][1 \;\; (S_Z + d_2) \;\; -(S_z + e_2)]^T = 0 \tag{28} $$

where

$$ \mathbf{M} = (a_1 + S_X)\mathbf{I_1} + S_Y\mathbf{J}_2 - (b_1 + S_x)\mathbf{Ti_1} - S_y\mathbf{Tj_2} - \mathbf{P} $$

Because the 3 by 3 matrix $[\mathbf{M} \quad \mathbf{K}_2 \quad \mathbf{Tk_2}]$ includes only variables ϕ and ψ, the input-output equation can be derived from the determinant of $[\mathbf{M} \quad \mathbf{K}_2 \quad \mathbf{Tk_2}]$ being zero. All nine coefficients as in Equation (1) are derived as

$$ A = (a_1 + S_X)\cos\alpha_1\sin\gamma_1 + (b_1 + S_x)\sin\alpha_1\cos\gamma_1 $$
$$ B = -g\sin\alpha_1\sin\gamma_1 + h\sin\alpha_1\cos\beta\sin\gamma_1 - S_Y\sin\gamma_1 + S_y\sin\alpha_1\cos\beta $$
$$ C = -h\cos\alpha_1\sin\beta\sin\gamma_1 - S_y\cos\alpha_1\sin\beta $$
$$ D = g\sin\alpha_1\cos\beta\sin\gamma_1 - h\sin\alpha_1\sin\gamma_1 + S_Y\cos\beta\sin\gamma_1 - S_y\sin\alpha_1 $$
$$ E = (a_1 + S_X)\cos\alpha_1\cos\beta\sin\gamma_1 - f\sin\alpha_1\sin\beta\sin\gamma_1 + (b_1 + S_x)\sin\alpha_1\cos\beta\cos\gamma_1 $$
$$ F = (a_1 + S_X)\sin\alpha_1\sin\beta\sin\gamma_1 - f\cos\alpha_1\cos\beta\sin\gamma_1 - (b_1 + S_x)\cos\alpha_1\sin\beta\cos\gamma_1 $$
$$ G = g\sin\alpha_1\sin\beta\cos\gamma_1 + S_Y\sin\beta\cos\gamma_1 $$
$$ H = (a_1 + S_X)\cos\alpha_1\sin\beta\cos\gamma_1 + f\sin\alpha_1\cos\beta\cos\gamma_1 - (b_1 + S_x)\sin\alpha_1\sin\beta\sin\gamma_1 $$
$$ I = -(a_1 + S_X)\sin\alpha_1\cos\beta\cos\gamma_1 - f\cos\alpha_1\sin\beta\cos\gamma_1 - (b_1 + S_x)\cos\alpha_1\cos\beta\sin\gamma_1 \tag{29} $$

Example 1: The parameters of an RPSPR linkage are listed as: a_1=5, $\alpha_1 = -60^o$, $S_X = 8$, $S_Y = 4$, $b_1 = 8$, $\gamma_1 = 25^o$, $S_x = 3$, $S_y = 2$, f=25, g=10, h=8, and $\beta = 20^o$.

Sol: The common approach in analyzing this linkage is to find the output angle for each given input angle. As shown in Figure 7, the results are obtained for input angle=1, 2, .. , 360 degrees, and Equation (2) was solved 360 times. Finally, the linkage can be judged as double-rocker by observing the curves, and the mobility regions of input link are around -20~66 and 96~205.

The technique developed in this article is then applied to analyze this linkage. None of the coefficients in Equation (1) or (6) are zero for this general RPSPR, and concise criteria do not exist. The mobility regions are determined numerically.

Step 1: Use Equations (29) to calculate all nine coefficients appeared in Equation (1).

Step 2: Regarding the input link, calculate C_i and derive the equation $\Delta_1(\phi) = 0$ by following Equations (6). By combining $\Delta_1(\phi) = 0$ and unit circle, all $\phi_{\lim}$ are found as 66.7322 (-), 95.6806 (+), 205.1123 (-), and 339.6900 (+). Meanwhile, (+) and (-) represent the signs of $d\Delta_1/d\phi|_{\phi=\phi_{\lim}}$. The mobility regions are then 95.6806~205.1123 and -20.3100~66.7322.

Step 3:For the output link, calculate $\hat{C}_i$ by following Equations (9). It is a crank since there is no real solution for $\Delta_2 = 0$ and Δ_2 is always positive.

Step 4:The type of the linkage is a double-rocker and it becomes a crank-rocker if both input and output links are swapped.

Several evident advantages of using present technique are as follows: the computation time

is reduced extensively, the limiting positions and mobility region can be found out precisely, and the type of each concerned link can be determined easily without observing any curves.

The RPSPR linkage becomes an RPSC if both P_2 and R_2 axes are coincident, and parameters b_1, γ_1, and S_y are all zero. Regarding a special case that both input and output axes are parallel or $\beta = 0$, the coefficients B, C, D, F, G, C_3, C_4, $\hat{C}_3$, and $\hat{C}_4$ are all zero. Since $C_1 - C_2 = (f \sin\alpha_1)^2 \geq 0$, the criteria for input link being a crank are just Equations (14) and are

$$\left(S_x{}^2 - f^2 - (a_1 + S_X)^2\right) - 2f(a_1 + S_X) \geq 0$$
$$\left(S_x{}^2 - f^2 - (a_1 + S_X)^2\right) + 2f(a_1 + S_X) \geq 0$$

Both inequalities can be combined to get the criterion $S_x \geq f + a_1 + S_X$. Similarly, the output link can make fully rotation if either $S_x \geq f + a_1 + S_X$ or $f \geq S_x + a_1 + S_X$ is satisfied.

5. Analysis of RSSR linkage

The RSSR linkage shown in Figure 8 is then analyzed. The lengths of input, output, and coupler links are defined as a, b, and c. The derivation as for the RPSPR linkage can be followed to derive the input-output equation. Some coefficients in Equation (6) are listed as

$$C_1 = 4a^2\left(b^2\cos^2\beta - h^2\sin^2\beta\right)$$
$$C_2 = 4a^2\left(b^2 - f^2\right)$$
$$C_3 = -8a^2 fh\sin\beta$$
$$C_4 = 2\left(-4ab^2 g\cos\beta\sin\beta + 2ah\sin\beta\cdot I\right)$$
$$C_5 = 2\left(-4ab^2 f + 2af\cdot I\right)$$
$$C_6 = 4b^2g^2\sin^2\beta + 4b^2f^2 - I^2$$
$$I = a^2 + b^2 - c^2 + f^2 + g^2 + h^2 - 2gh\cos\beta \qquad (30)$$

Although finding the mobility regions numerically is necessary for general RSSR, type determination criteria can be derived easily for six special RSSR linkages, such as planar four-bar, spherical four-bar, simply skewed four-bar and for conic becoming a circle.

If a planar four-bar is considered, the values of g, h, β, C_3, and C_4 are all zero. Both Equations (14-1) and (14-2) are the criteria for the input link being a crank and become

$$(a + b + c - f)(-a + b + c + f)(a + b - c - f)(a - b + c - f) \geq 0$$
$$(a + b + c + f)(a - b + c + f)(a + b - c + f)(-a + b + c - f) \geq 0 \qquad (31)$$

If the linkage can be connected, both inequalities can be simplified as

$$(a + b - c - f)(a + c - b - f) \geq 0$$
$$a + f \leq b + c \qquad (32)$$

Further analysis can lead to that either link length a or f is the minimum and $\ell_{min} + \ell_{max} \leq \ell_1 + \ell_2$. Grashof's rule can then be proved. Besides, similar derivation is also applicable to the case $\beta = 0$.

For spherical four-bar or $f = 0$, the coefficients in Equation (30) become $C_2 - C_1 = 4a^2\sin^2\beta\left(b^2 + h^2\right) > 0$ and $C_3 = C_5 = 0$. Hence, the criteria for the existence of crank are again $C_1 + C_6 + C_4 \geq 0$ as well as $C_1 + C_6 - C_4 \geq 0$.

For $h = 0$ and $f = b\sin\beta$, the conic curve becomes a circle since B=D=G=0, $C_1 = C_2$ and $C_3 = 0$. The input link is a crank if Equation (23) is satisfied.

Regarding the simply skewed four-bar g=h=0, the coefficients of conic curve are $C_3 = C_4 = 0$

and $C_1 - C_2 = 4a^2\left(f^2 - b^2\sin^2\beta\right)$. The criteria are just Grashof's rule when $f \geq b|\sin\beta|$ or $C_1 - C_2 \geq 0$. If $f < b|\sin\beta|$, at least one of Equations (19) has to be satisfied and they become

$$\begin{aligned}
&-2\left(a^2b^2 + a^2c^2 + a^2f^2 + b^2c^2 + b^2f^2 + c^2f^2\right)\sin^2\beta \\
&\quad + \left(a^4 + b^4 + c^4 + f^4\right)\sin^2\beta + 4a^2b^2\sin^4\beta + 4c^2f^2 \leq 0 \\
&f^2(a^2 - b^2 - c^2 + f^2)^2 - 4a^2(b^2\sin^2\beta - f^2)^2 \geq 0 \\
&-a^4 + (2b^2 + 2f^2 + 2c^2 - 8b^2\sin^2\beta)a^2 + 4b^2f^2 - (f^2 + b^2 - c^2)^2 \geq 0
\end{aligned} \tag{33}$$

Besides, similar derivation can be applied to the case when $h = \cos\beta = 0$. The linkages that are analyzed and have concise criteria for type determination are also listed in Table 2.

6. Linkage with prismatic output

If the output joint becomes prismatic, the general form of input-output equation is

$$\left(\overline{A}h^2 + \overline{B}h + \overline{C}\right)\cos\phi + \left(\overline{D}h^2 + \overline{E}h + \overline{F}\right)\sin\phi + \overline{G}h^2 + \overline{H}h + \overline{I} = 0 \tag{34}$$

The function Δ_ϕ, similar to Δ_1, is derived as

$$\Delta_\phi = \left(\overline{B}\cos\phi + \overline{E}\sin\phi + \overline{H}\right)^2 - 4\left(\overline{A}\cos\phi + \overline{D}\sin\phi + \overline{G}\right)\left(\overline{C}\cos\phi + \overline{F}\sin\phi + \overline{I}\right) \geq 0 \tag{35}$$

The coefficients as in Equations (6) become

$$\begin{aligned}
&\overline{C_1} = \overline{B}^2 - 4\overline{A}\,\overline{C} && \overline{C_2} = \overline{E}^2 - 4\overline{D}\,\overline{F} \\
&\overline{C_3} = 2\overline{B}\,\overline{E} - 4\overline{C}\,\overline{D} - 4\overline{A}\,\overline{F} && \overline{C_4} = 2\overline{B}\,\overline{H} - 4\overline{A}\,\overline{I} - 4\overline{C}\,\overline{G} \\
&\overline{C_5} = 2\overline{E}\,\overline{H} - 4\overline{D}\,\overline{I} - 4\overline{F}\,\overline{G} && \overline{C_6} = \overline{H}^2 - 4\overline{G}\,\overline{I}
\end{aligned} \tag{36}$$

The function Δ_h related to the prismatic output is a quartic equation

$$\Delta_h \equiv (\overline{A}h^2 + \overline{B}h + \overline{C})^2 + (\overline{D}h^2 + \overline{E}h + \overline{F})^2 - (\overline{G}h^2 + \overline{H}h + \overline{I})^2 \geq 0 \tag{37}$$

If an RSSP linkage shown in Figure 9 is to be analyzed, the input-output equation can be modified from that of RSSR linkage. Parameters b and ψ are both zero. The point B, also origin of frame $x_0 - y_0 - z_0$, slides on a fixed link. The offset $|P_2B| = h$ becomes a variable. Some related coefficients are thus

$$\begin{aligned}
&\overline{A} = \overline{C} = \overline{D} = \overline{E} = 0 && \overline{B} = -2a\sin\beta \\
&\overline{F} = -2af && \overline{G} = 1 \\
&\overline{H} = -2g\cos\beta && \overline{C_1} = 4a^2\sin^2\beta \\
&\overline{C_2} = \overline{C_3} = 0 && \overline{C_5} = 8af \\
&\overline{C_4} = 2\overline{B}\,\overline{H} - 4\overline{A}\,\overline{I} - 4\overline{C}\,\overline{G} = 4ag\sin 2\beta
\end{aligned} \tag{38}$$

Although both terms $\overline{C_2}$ and $\overline{C_3}$ are zero, the quartic discriminants have to be applied to derive the criteria for type determination. For the special case $g = 0$, $\sin\beta = 0$, or $\cos\beta = 0$, Equations (14) are again the criteria for the input link since $\overline{C_3} = \overline{C_4} = 0$ and $\overline{C_1} > \overline{C_2}$. Meanwhile, the coefficients of both terms h and h^3 in Equation (37) are zero for $g = 0$ or $\cos\beta = 0$, and the limiting positions for the prismatic joint are easy to derive.

For the RSSP linkage with $f = 0$, the conic equation becomes

$$\overline{C_1}X^2 + \overline{C_4}X + \overline{C_6} \geq 0 \tag{39}$$

This belongs to the special case $C_3 = C_5 = 0$. Replacing $\overline{C_2}$ and $\overline{C_5}$ by $\overline{C_1}$ and $\overline{C_4}$ are necessary as proposed in Figure 5, and Equations (14)* become

$$\overline{C_1}+\overline{C_6}+\overline{C_4}\geq 0 \quad \text{and} \quad \overline{C_1}+\overline{C_6}-\overline{C_4}\geq 0 \tag{40}$$

Since $\overline{C_1}>\overline{C_2}$, Equations (19)* have to be considered as well. All these four special RSSP linkages and corresponding concise criteria are also listed in Table 2.

7. Conclusion

For any bimodal linkages of which the input-output equation can be formulated as Equation (1) or (34), the limiting positions are found by solving a conic curve and a unit circle as proposed in Section 2. The mobility regions can then be figured out efficiently with considering the signs of the first differentiation at limiting positions.

The concise criteria to determine the type for a selective group of bimodal linkages have been derived and can be treated as the generalized Grashof's rule. The feature of this group is clearly defined as one axis of the conic curve passing through the origin. Whether a considered linkage belongs to this selective group can be judged easily from the coefficients of input-output equation. In addition to the well-known planar and spherical four-bar linkages, at least nine linkages belonging to this selective group are illustrated in this article. The corresponding type determination criteria are all listed in Table 2.

The results in Section 2 and Section 3 can be integrated as proposed in Figure 5 to develop computer software for designing bimodal linkages. For any concerned linkage, the input-output equation can be derived by following the techniques for RPSPR and RSSR linkages. Thereafter, the program can numerically figure out the mobility regions. Most of all, the type determination criteria can be derived symbolically and straightforwardly if one axis of the resultant conic curve passes through the origin.

References

1. Ting, K.L. and Dou, X. Branch, Mobility Criteria, and Classification of RSSR and Other Bimodal Linkages. ASME Mechanisms Conference: Mechanism Synthesis and Analysis, 1994, DE-70, 303-310.
2. Paul, B. A Reassessment of Grashof's Criterion. Transactions of the ASME, Journal of Mechanical Design, 1979, 101, 515-518.
3. Chiang, C.H. Kinematics of Spherical Mechanisms. Cambridge University Press, 1988.
4. Bottema, O., The Motion of the Skew Four-Bar, Journal of Mechanisms, 1971, 6, 69-79.
5. Zhang, W. and Zhang D. Conditions of Crank Existence for a Particular Case of the RSSR Linkage. Mechanism and Machine Theory, 1993, 28, 845-850.
6. Chung, W. Mobility Analysis of RSSR Mechanisms by Working Volume. ASME Journal of Mechanical Design, 2005, 127, 156-159.
7. Freudenstein, F. and Kiss I. Type Determination of Skew Four-Bar Mechanisms. Transaction of the ASME: Journal of Engineering for Industry, 1969, 91, 220-224.
8. Freudenstein, F. and Primrose, E. On the Criteria for the Rotatability of the Cranks of Skew Four-Bar Linkage. ASME Journal of Engineering for Industry, 1976, 98, 1285-1288.
9. Nolle, H. Ranges of Motion Transfer by the R-G-G-R Linkage. Journal of Mechanisms, 1968, 4, 145-157.
10. Kazerounian, K. and Solecki, R. Mobility Analysis of General Bi-Modal Four-Bar Linkages Based on Their Transmission Angle. Mechanism and Machine Theory, 1993, 28, 437-445.
11. Williams, R.L. and Reinholtz, C. F. Mechanism Link Rotatability and Limit Position Analysis Using Polynomial Discriminants. ASME Journal of Mechanisms, Transmissions, and Automation in Design, 1987, 109, 178-182.
12. Harrisberger, L. Space Crank Mechanisms, Machine Design, 1964, 36, pp.170-175.
13. Gupta V. and Radcliffe C. Mobility Analysis of Plane and Spatial Mechanisms. Transaction of the ASME: Journal of Engineering for Industry, 1971, 93, 125-130.

14. Suh C. H. and Radcliffe C. W., Kinematics and Mechanisms Design, 1978, John Wiley & Sons.
15. Angeles, J. and Bernier A General Method of Four-Bar Linkage Mobility Analysis. ASME Journal of Mechanisms, Transmissions, and Automation in Design, 1987, 109, 197-203.
16. Mallik, A.K. Mobility Analysis and Type Identification of Four-Link Mechanisms. ASME Journal of Mechanical Design, 1994, 116, 629-633.
17. Rastegar, J. and Tu, Q. Approximated Grashof-Type Movability Conditions for RSSR Mechanisms with Force Transmission Limitations. Transactions of the ASME, Journal of Mechanical Design, 1992, 114, 74-81.
18. DasGupta, A. Mobility Analysis of a Class of RPSPR Kinematic Chains. ASME Journal of Mechanical Design, 2004, 126, 71-78.
19. Denavit, J. and Hartenberg, R.S. A Kinematic Notation for Lower-Pair Mechanism Based on Matrices. Journal of Applied Mechanics, 1955, 22, 215-221.
20. Craig, J.J. Introduction to Robotics: Mechanics and Control, 2005, Addison-Wesley Publishing Company.

Table 1 Properties of T_1 、T_2 and T_3 at four regions

	T_1	T_2	T_3
I	+	+	+
II	-	I	-
III	+	-	-
IV	+	+	-

+: positive -: negative I: imaginary number

Table 2: Some linkage with concise criteria for type determination

Linkage	Dimension	Criteria	Remark
RPSC	$\sin\beta = 0$	Eq (14)	
RSSR	g=h=0 $\sin\beta = 0$	Eq (14)	planar four-bar
	$\sin\beta = 0$	Eq (14)	
	f=0	Eq (14)	spherical four-bar
	$h = 0 \quad f = b\sin\beta$	Eq (23)	conic is a circle
	g=h=0	Eq (14) & (19)	RSSR with zero offsets
	$h = \cos\beta = 0$	Eq (14) & (19)	
RSSP	g=0	Eq (14)	
	$\cos\beta = 0$	Eq (14)	
	$\sin\beta = 0$	Eq (14)	
	f=0	Eq (14)* & (19)*	

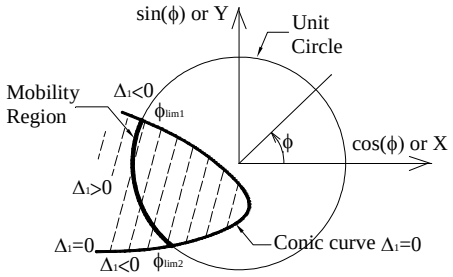

Figure 1 Illustration of finding mobility region

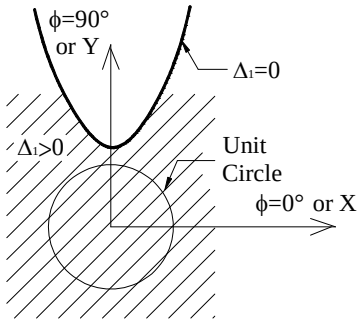

(a). $-C_5 \geq 0$ and $(C_2 + C_6)/(-C_5) \geq 1$

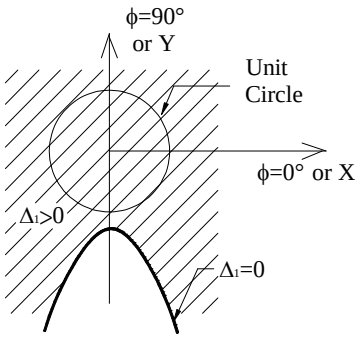

(b) $-C_5 \leq 0$ and $(C_2 + C_6)/(-C_5) \leq -1$

Figure 2 Two cases for $C_1 \geq C_2$

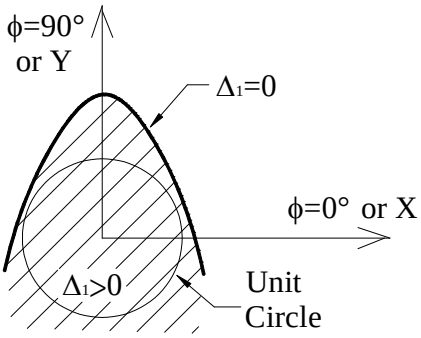

(a). $-C_5 \geq 0$ and $(C_2 + C_6)/(-C_5) \geq 1$

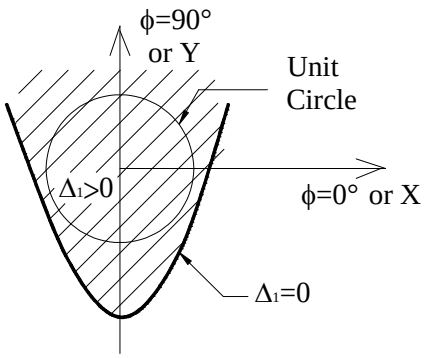

(b) $-C_5 \leq 0$ and $(C_2 + C_6)/(-C_5) \leq -1$

Figure 3 Two cases for $C_1 < C_2$

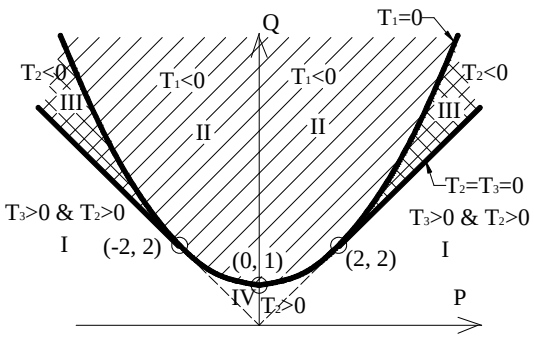

Figure 4 Analysis of constraint functions T_1, T_2, and T_3

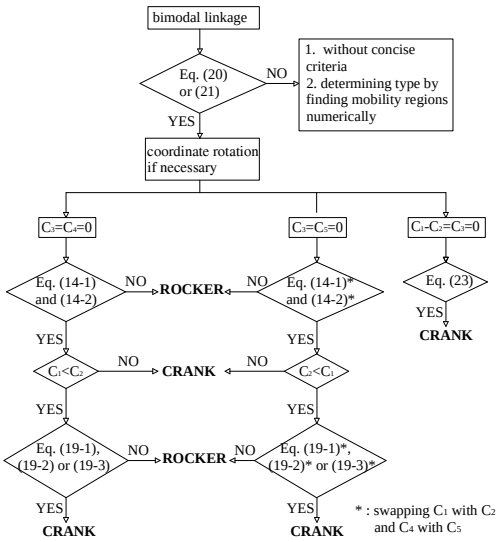

Figure 5 Flowchart for deriving type determination criteria

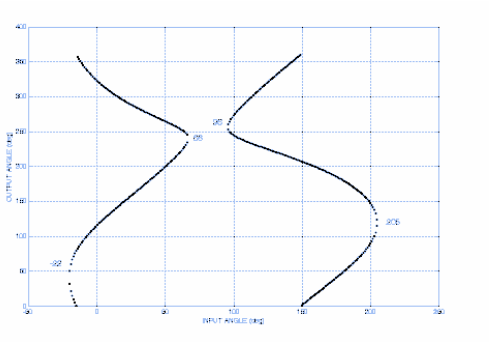

Figure 7 Output angle versus input angle

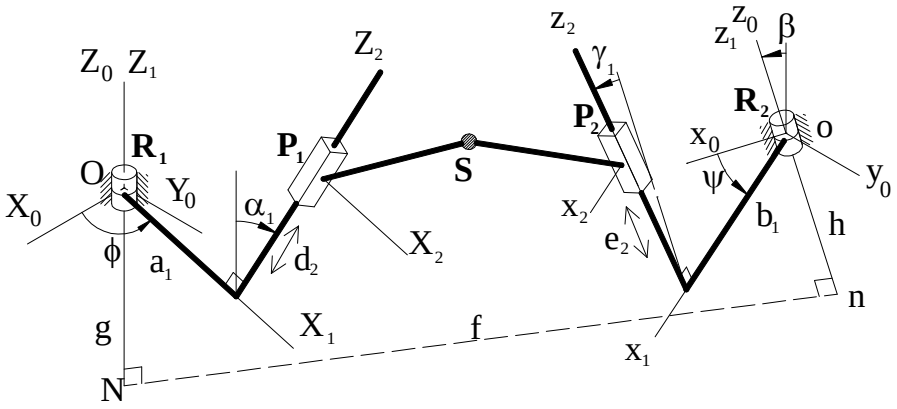

Figure 6 Illustration of RPSPR linkage

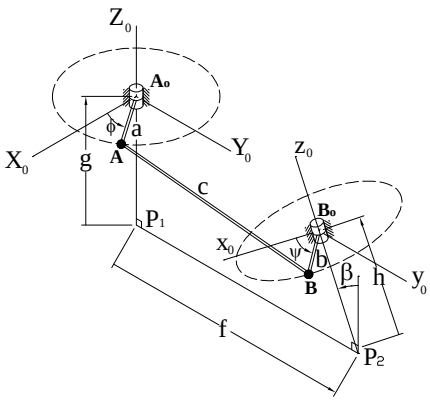

Figure 8 Illustration of RSSR linkage

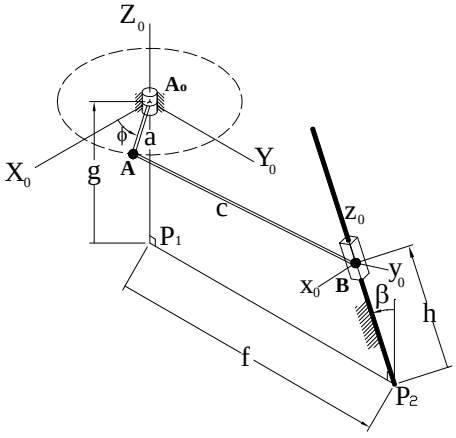

Figure 9 Illustration of RSSP linkage